

# Phase Structure of 2-Flavor Quark Matter: Heterogeneous Superconductors

Sanjay Reddy and Gautam Rupak

*Theoretical Division, Los Alamos National Laboratory,  
Los Alamos, NM 87545*

We analyze the free energy of charge and color neutral 2-flavor quark matter within the BCS approximation. We consider both the homogeneous gapless superconducting phase and the heterogeneous mixed phase where normal and BCS superconducting phases coexist. We calculate the surface tension between normal and superconducting phases and use it to compare the free energies of the gapless and mixed phases. We find that the mixed phase is energetically favored.

PACS numbers: PACS numbers(s):12.38.-t,26.60.+c,97.60.Jd

## I. INTRODUCTION

At high baryon density, we expect on general grounds that nuclear matter will undergo a phase transition to the de-confined quark phase. Although the nature of this transition and its location remain unclear, theory suggests that the quark phase is likely to be a color superconductor. This expectation is several decades old [1, 2]. Recent work based on effective models for the quark-quark interaction predict a superconducting gap  $\Delta \simeq 100$  MeV for a quark chemical potential  $\mu \simeq 400$  MeV [3, 4] and has generated renewed interest in the field. The pairing or BCS (Bardeen-Cooper-Schrieffer) instability is strongest in the spin-zero, color and flavor antisymmetric channel naturally resulting in pairing between quarks of different flavors. Any source of flavor symmetry breaking will induce a stress on the paired state since it will act to move the Fermi surfaces of the different flavors apart. There has been much recent interest in how this will affect the ground state properties of quark matter. In this work we investigate the role of the large isospin breaking induced by electromagnetism in 2 flavor quark matter.

In the absence of any flavor symmetry breaking the ground state of bulk three flavor quark matter is expected to be the Color-Flavor-Locked state [5]. In this phase, all nine quarks participate in pairing and the  $SU(3)_{\text{color}} \times SU(3)_L \times SU(3)_R \times U(1)_B$  symmetry of QCD is broken down to the global diagonal  $SU(3)$  symmetry. Chiral symmetry breaking results in light pseudo-Goldstone modes with the quantum numbers of the pions, kaons and eta's. This phase is neutral with respect to electric and color charge as it contains equal numbers of up, down and strange quarks. A finite strange quark mass breaks flavor symmetry. For small values of the strange quark mass ( $m_s \ll \Delta$ ) the stress on the CFL state is resolved via a novel mechanism wherein the light pseudo-Goldstone modes condense [6, 7]. Bedaque and Schafer have shown that the stress induced by the strange quark mass can result in the condensation of neutral kaons in the CFL state [6]. At intermediate values of the strange quark mass corresponding to  $m_s^2/\mu \simeq \Delta$ , the situation is less clear. Recent, calculations suggest the possible existence of a color-flavor locked phase with non-trivial gapless quark excitations [8].

In this article we study the case where the (effective) strange quark mass is large compared to the quark chemical potential. Here no strange quarks are present and the excess charge of the up and down quarks is neutralized by electrons, which in turn induces a splitting  $\delta\mu = (\mu_u - \mu_d)/2$  between the up and down quark chemical potentials. If  $\delta\mu$  is large compared to the pairing energy, the pairing breaks down and the normal state is favored. At intermediate values, interesting new phases are possible and have been previously suggested. These include the homogeneous gapless superconducting phase [9] (the gapless superconducting phase is also called the Sarma or breached phase[10]) and the heterogeneous mixed phase where normal and BCS superconducting phase coexist [11, 12]. Although we do not study it in this work, we note that there exists a small interval in  $\delta\mu/\Delta$  where crystalline superconductivity could be favored [13]. This crystalline phase, which is also called the Larkin, Ovchinnikov, Fulde and Ferrel (LOFF) phase, is characterized by a spatial variation of  $\Delta$  on a scale  $1/\delta\mu$ . The mixed phase that we consider here shares some features with the LOFF phase: spatial variation of  $\Delta$  and crystalline structure. In the mixed phase electric charge neutrality is satisfied as a global constraint- a positively charged BCS phase coexists and neutralizes the negatively charged normal phase. This charge separation leads to long-range order and crystalline structure at low temperature[14]. The description and competition between the mixed and gapless phases is the subject of this article. Finally, we shall find that for the model parameters we employed, the heterogeneous mixed phase is favored.

We will begin by deriving the free energy of color and charge neutral matter containing light (up and down) quarks and electrons in Sec. II. In concordance with earlier findings we show the existence of two stable and neutral bulk ground states: the homogeneous gapless state and the heterogeneous mixed phase. In Sec. IV, we calculate the surface tension between the normal and superconducting phases in the mixed phase. We will then use these results to compare the free energies of the homogeneous and heterogeneous superconducting phases in Sec. V. Finally in Sec. VI we conclude with a discussion of our results and explore some of its consequences for astrophysics of neutron stars that may contain quark matter.

## II. FREE ENERGY

We consider a system of massless electrons, and two degenerate light quarks (up and down), with three color degrees of freedom at finite quark chemical potential  $\hat{\mu} = \mu + \mu_Q Q + \mu_8 T_8 + \mu_3 T_3$ . We have written the quark chemical potential in terms of the baryon chemical potential ( $\mu = \mu_B/3$ ), the electric charge chemical potential ( $\mu_Q$ ) and the color chemical potentials ( $\mu_3$  and  $\mu_8$ ). The electric charge matrix and the color matrices are defined below.

$$Q = \begin{pmatrix} \frac{2}{3} & 0 \\ 0 & -\frac{1}{3} \end{pmatrix} = \frac{1}{6} + \frac{1}{2}\tau_3, \quad T_3 \equiv 2\lambda_3 = \begin{pmatrix} 1 & 0 & 0 \\ 0 & -1 & 0 \\ 0 & 0 & 0 \end{pmatrix}, \quad T_8 \equiv 2\sqrt{3}\lambda_8 = \begin{pmatrix} 1 & 0 & 0 \\ 0 & 1 & 0 \\ 0 & 0 & -2 \end{pmatrix}. \quad (1)$$

It is convenient to write the quark chemical potential as

$$\mu = \mu_0 + \delta\mu \tau_3 + \mu_3 T_3 + \mu_8 T_8 \quad (2)$$

where  $\mu_0 = \mu + \mu_Q/6$  and  $\delta\mu = \mu_Q/2$ . The Pauli matrices  $\tau_i$ 's act in flavor space and the Gell-Mann matrices  $\lambda_i$ 's act in color space.

We model the pairing interaction by a four-quark operator with the quantum numbers of the single gluon exchange interaction. As Eq. 3 shows, one gluon exchange is attractive in the color anti-symmetric channel and repulsive in the symmetric channel.

$$-(\bar{\Psi}\gamma_\mu\lambda_A\Psi)(\bar{\Psi}\gamma^\mu\lambda_A\Psi) = (\bar{\Psi}_\alpha\gamma_\mu\Psi_\beta)(\bar{\Psi}_\gamma\gamma^\mu\Psi_\delta) \left[ \frac{1}{3}(\delta_{\alpha\beta}\delta_{\gamma\delta} - \delta_{\alpha\delta}\delta_{\beta\gamma}) - \frac{1}{6}(\delta_{\alpha\beta}\delta_{\gamma\delta} + \delta_{\alpha\delta}\delta_{\beta\gamma}) \right], \quad (3)$$

where the first term corresponds to the attractive color antisymmetric  $\bar{\mathbf{3}}$  channel. For pairing, we only consider the attractive channel. Further, we consider the pairing to be in the spin zero,  $S$ -wave and flavor antisymmetric channel. So, the four-quark operator is taken to be

$$g(\bar{\Psi}_\alpha\gamma_5\tau_2\Psi_\beta^c)(\bar{\Psi}_\gamma^c\gamma_5\tau_2\Psi_\delta)(\delta_{\alpha\gamma}\delta_{\beta\delta} - \delta_{\alpha\delta}\delta_{\beta\gamma}), \quad (4)$$

$$\Psi^c = C\bar{\Psi}^T = i\gamma_2\Psi^*, \quad \bar{\Psi}^c = \Psi^T C = i\Psi^T\gamma_2\gamma_0.$$

Using the 2SC ansatz  $\bar{\Psi}_\alpha^c\gamma_5\tau_2\Psi_\beta = i\Delta\varepsilon_{\alpha\beta 3}/(4g)$  (where blue quarks remain unpaired) for the BCS gap  $\Delta$  in mean field approximation, we get for the quark Lagrangian

$$\begin{aligned} \mathcal{L} + \mu N &= \bar{\Psi}(i\cancel{\partial} + \gamma_0\mu - m)\Psi + g(\bar{\Psi}_\alpha\gamma_5\tau_2\Psi_\beta^c)(\bar{\Psi}_\gamma^c\gamma_5\tau_2\Psi_\delta)(\delta_{\alpha\gamma}\delta_{\beta\delta} - \delta_{\alpha\delta}\delta_{\beta\gamma}) \\ &= \bar{\Psi}^{(b)}(i\cancel{\partial} + \gamma_0\mu_b)\Psi^{(b)} - \frac{\Delta^2}{4g} - \frac{1}{2}\bar{\Psi}_i^{(rg)}M_{ij}\Psi_j^{(rg)}, \\ \mu_b &= \mu_0 - 2\mu_8 + \delta\mu\tau_3, \\ \bar{\Psi}^{(rg)} &= (\bar{\Psi} \quad \bar{\Psi}^c), \\ M &= \begin{pmatrix} i\cancel{\partial} - m + \gamma_0(\mu_0 + \delta\mu\tau_3 + \mu_3\sigma_3 + \mu_8) & -\gamma_5\tau_2\sigma_2\Delta \\ \gamma_5\tau_2\sigma_2\Delta & i\cancel{\partial} - m - \gamma_0(\mu_0 + \delta\mu\tau_3 + \mu_3\sigma_3 + \mu_8) \end{pmatrix}. \end{aligned} \quad (5)$$

The Dirac spinor fields  $\Psi^{(b)}$ ,  $\Psi^{(rg)}$  represents the blue, and red-green quark fields respectively. The Pauli matrices  $\tau_i$ 's act in flavor space, and  $\sigma_i$ 's act in color space. Integrating over the fermionic variables in the partition function, the free energy for a constant gap field  $\Delta$  is given by

$$\begin{aligned} \Omega_{2SC}(\Delta) &= \frac{\Delta^2}{4g} + 2\sum_{\pm} \int \frac{d^3p}{(2\pi)^3} (\sqrt{\mathbf{p}^2 + m^2} - \mu_b \pm \delta\mu)\theta(\mu_b \mp \delta\mu - \sqrt{\mathbf{p}^2 + m^2}) \\ &\quad + \frac{i}{2} \int \frac{d^4p}{(2\pi)^4} \text{Tr} \log G(p) - \frac{\mu_Q^4}{12\pi^2} + C, \\ G(p) &= \begin{pmatrix} \not{p} - m + \gamma_0(\mu_0 + \delta\mu\tau_3 + \mu_3\sigma_3 + \mu_8) & -\gamma_5\tau_2\sigma_2\Delta \\ \gamma_5\tau_2\sigma_2\Delta & \not{p} - m - \gamma_0(\mu_0 + \delta\mu\tau_3 + \mu_3\sigma_3 + \mu_8) \end{pmatrix}, \end{aligned} \quad (6)$$

where we added the contribution to the free energy from the electrons with chemical potential  $\mu_e = -\mu_Q$ . The constant  $C$  is fixed such that  $\Omega_{2SC}(\Delta = 0)$  gives the free energy of the non-interacting system of electrons and quarks.

A straightforward calculation using the identities [11]

$$\text{Tr} \log \begin{pmatrix} A & B \\ C & D \end{pmatrix} = \text{Tr} \log (-BC + BDB^{-1}A), \quad (7)$$

$$\int \frac{d^4 p}{(2\pi)^4} \log [(p_0(1+i\delta)+a)^2 - b^2] = i \int \frac{d^3 p}{(2\pi)^3} [(a+b)\theta(a+b) + (a-b)\theta(a-b)],$$

gives

$$\begin{aligned} \Omega_{2\text{SC}}(\Delta) = & -\frac{\mu_Q^4}{12\pi^2} + \frac{\Delta^2}{4g} - 2 \int \frac{d^3 p}{(2\pi)^3} \sum_{\pm} \left[ (\delta\mu + \mu_3 + \sqrt{\Delta^2 + \varepsilon_{\pm}^2})\theta(\delta\mu + \mu_3 + \sqrt{\Delta^2 + \varepsilon_{\pm}^2}) \right. \\ & + (\delta\mu + \mu_3 - \sqrt{\Delta^2 + \varepsilon_{\pm}^2})\theta(\delta\mu + \mu_3 - \sqrt{\Delta^2 + \varepsilon_{\pm}^2}) \\ & + (\delta\mu - \mu_3 + \sqrt{\Delta^2 + \varepsilon_{\pm}^2})\theta(\delta\mu - \mu_3 + \sqrt{\Delta^2 + \varepsilon_{\pm}^2}) \\ & \left. + (\delta\mu - \mu_3 - \sqrt{\Delta^2 + \varepsilon_{\pm}^2})\theta(\delta\mu - \mu_3 - \sqrt{\Delta^2 + \varepsilon_{\pm}^2}) \right] + C, \end{aligned} \quad (8)$$

$$\varepsilon_{\pm}(p) = \sqrt{\mathbf{p}^2 + m^2} \pm (\mu_0 + \mu_8).$$

The momentum integrals are evaluated with a cutoff  $\Lambda$ . The coupling  $g(\Lambda)$  is determined by requiring a BCS gap  $\Delta_0 = 100$  MeV at  $\mu = 350$  MeV and  $\mu_Q = 0 = \mu_3 = \mu_8$ .

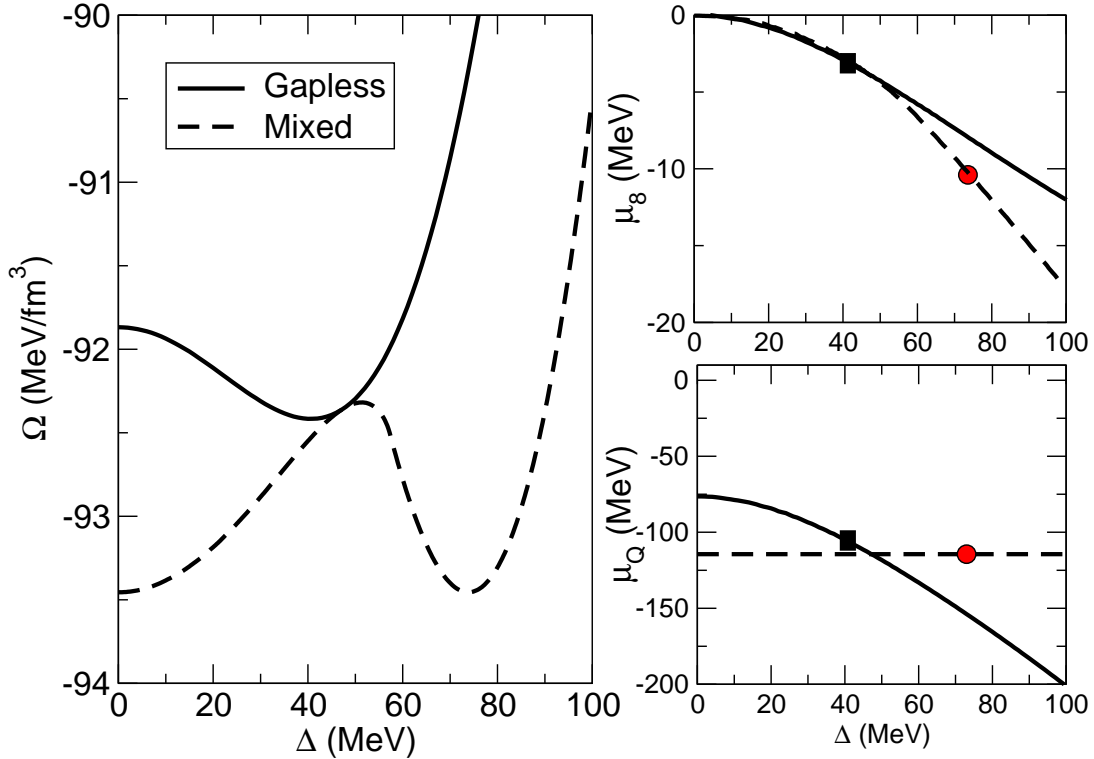


FIG. 1: Free energy curves for the gapless (solid) and mixed phases (dashed) as a function of  $\Delta$  for  $\mu = 350$  MeV. The gapless free energy is characterized by the imposition of local electric and color charge neutrality while in the mixed phase electric charge neutrality is imposed globally. These requirements induce chemical potentials  $\mu_Q$  and  $\mu_8$  and are shown in the right panels. The filled dots and rectangles indicate the locations of the mixed and gapless ground states.

Bulk matter is neutral with respect to electric and color charge. In what follows we investigate both homogeneous and heterogeneous phases. For the former, color and electric charge neutrality is a local condition. In this case, for a given baryon chemical potential  $\mu$ , we require that

$$-\frac{\partial \Omega_{2\text{SC}}}{\partial \mu_3} = 0 = -\frac{\partial \Omega_{2\text{SC}}}{\partial \mu_8}, \quad -\frac{\partial \Omega_{2\text{SC}}}{\partial \mu_Q} = 0. \quad (9)$$

These sets of equations determine  $\mu_Q$ ,  $\mu_3$ ,  $\mu_8$  at any value of the gap  $\Delta$ . Simultaneously solving the above set of equations together with the gap equation  $\partial\Omega_{2SC}/\partial\Delta = 0$  determines the gapless states. Denoting the solutions as  $\tilde{\mu}_Q$ ,  $\tilde{\mu}_3$ ,  $\tilde{\mu}_8$  and  $\tilde{\Delta}$ , the free energy of the gapless phase is

$$\Omega_{\text{gapless}}(\mu) \equiv \Omega_{2SC}(\mu, \tilde{\mu}_Q, \tilde{\mu}_3, \tilde{\mu}_8, \tilde{\Delta}). \quad (10)$$

To construct the mixed phase comprising of normal and superconducting states, electric charge neutrality is imposed as a global constraint. In principle we could have imposed color neutrality as a global constraint in the heterogeneous phase. However, we expect the color Debye screening length,  $\lambda_{\text{Debye-color}}^{-1} \simeq \mu$ , to be short and comparable to the inter-particle distance in strong coupling. Under these conditions, color neutrality is essentially a local constraint. For normal and superconducting phases to co-exist they must satisfy the Gibbs criteria: for a given  $\mu$ , it requires equality of pressures at equal electric chemical potential. This results in the following condition

$$\Omega_{2SC}(\Delta = 0, \bar{\mu}_Q) = \Omega_{2SC}(\Delta_{\text{BCS}}, \bar{\mu}_Q), \quad (11)$$

which in turn uniquely determines  $\bar{\mu}_Q$  corresponding to the mixed phase. Global charge neutrality follows as long as the normal and superconducting phases have opposite electric charge. The volume fraction of the superconducting phase, which we call  $\chi$  is determined by the global constraint

$$\chi Q_{\text{SF}} + (1 - \chi) Q_{\text{Normal}} = 0, \quad (12)$$

where  $Q_{\text{SF}} = -\left. \frac{\partial\Omega_{2SC}(\Delta_{\text{BCS}}, \mu_Q)}{\partial\mu_Q} \right|_{\bar{\mu}_Q}$ ,  $Q_{\text{Normal}} = -\left. \frac{\partial\Omega_{2SC}(\Delta = 0, \mu_Q)}{\partial\mu_Q} \right|_{\bar{\mu}_Q}$ .

are the electric charge densities of the superconducting and normal phases respectively.

In Fig. 1, we show the free energy  $\Omega_{2SC}$  as a function of  $\Delta$  for  $\mu = 350$  MeV. The solid curve is for the case where electric and color charge neutrality conditions are imposed locally. The minimum seen at  $\Delta \simeq 40$  MeV corresponds to the gapless superconducting state described earlier. The dashed curve shows the free energy corresponding to the mixed phase. Here we have imposed only local color neutrality and determined the electric chemical potential using Eq. 11. Accordingly, it shows the existence of two degenerate minima corresponding to the normal and BCS superconducting states. The variation of the electric and color chemical potentials are also shown in Fig. 1. We find that  $\tilde{\mu}_3 = 0$  and  $|\tilde{\mu}_8| \ll |\bar{\mu}_Q| < |\mu_B|$ . Note that the  $\tilde{\mu}_8$  is small and proportional to  $\Delta$  since it is only through pairing that color neutrality is upset. On the other hand, the charge chemical potential  $\bar{\mu}_Q$  is large and non-vanishing even in the normal phase.

### III. COULOMB AND SURFACE ENERGY IN THE MIXED PHASE

The mixed phase free energy in Fig. 1 ignores finite size contributions arising due to Coulomb and surface energies associated with phase separation. If these effects are negligible, the results clearly indicate that the mixed phase is favored over the gapless phase. However, given the small difference in free energy between the gapless and mixed phases including these corrections becomes necessary. In Sec. IV we calculate the surface energy in the mixed phase. For now, we treat the surface tension as a parameter and study how it influences the free energy of the mixed phase.

The mixed phase can be subdivided into electrically neutral unit cells called Wigner-Seitz cells, as in the analysis of the inner crust of a neutron star where droplets of charged nuclear matter coexist with a negatively charged fluid of neutrons and electrons [15]. In the present context, each Wigner-Seitz cell will contain some positively charged superconducting quark matter and some negatively charged normal quark matter. Although at low temperature these unit cells form a Coulomb lattice, the interaction between adjacent cells can be neglected compared to the surface and Coulomb energy of each cell. In this Wigner-Seitz approximation, the surface and Coulomb energy per unit volume are fairly straightforward to calculate if the charge density in each phase is spatially uniform in each phase and if the surface thickness is small compared to the spatial extent of the Wigner-Seitz cell. We will examine both these requirements in greater detail in Sec. IV. For now we shall assume that these requirements are satisfied. In this case, the surface and Coulomb energies depend in general on the geometry and are given by [16]

$$E^S = \frac{d x \sigma}{r_0}, \quad (13)$$

$$E^C = 2\pi \alpha_{\text{em}} f_d(x) x (\Delta Q)^2 r_0^2, \quad (14)$$

where  $d$  is the dimensionality of the structure ( $d = 1, 2$ , and  $3$  correspond to Wigner-Seitz cells describing slab, rod and droplet configurations, respectively),  $\sigma$  is the surface tension,  $\Delta Q = Q_{\text{SF}} - Q_{\text{Normal}}$  is the charge density contrast between the two phases and  $\alpha_{\text{em}} = 1/137$  is the fine structure constant. The other factors appearing in Eqs. (13),(14) are:  $x$ , the fraction of the rarer phase which is equal to  $\chi$  where  $\chi \leq 0.5$  and  $(1 - \chi)$  where  $0.5 < \chi \leq 1$ ;  $r_0$ , the radius of the rarer phase (radius of drops or rods

and half-thickness of slabs); and  $f_d(x)$ , the geometrical factor that arises in the calculation of the Coulomb energy which can be written as

$$f_d(x) = \frac{1}{d+2} \left( \frac{2-d}{d-2} x^{1-2/d} + x \right). \quad (15)$$

The first step in the calculation is to evaluate  $r_0$  by minimizing the sum of  $E^C$  and  $E^S$ . The result is

$$r_0 = \left[ \frac{d \sigma}{4\pi \alpha_{em} f_d(x) (\Delta Q)^2} \right]^{1/3}. \quad (16)$$

We then use this value of  $r_0$  in Eqs. (13),(14) to evaluate the surface and Coulomb energy cost per unit volume

$$E^S + E^C = \frac{3}{2} (4\pi \alpha_{em} d^2 f_d(x) x^2)^{1/3} (\Delta Q)^{2/3} \sigma^{2/3}. \quad (17)$$

This equation allows us to include the free energy cost associated with the Coulomb field and surface. After calculating the surface tension in Sec. IV we will return to an analysis of the free energy competition between gapless and mixed phases in Sec. V.

#### IV. SURFACE TENSION

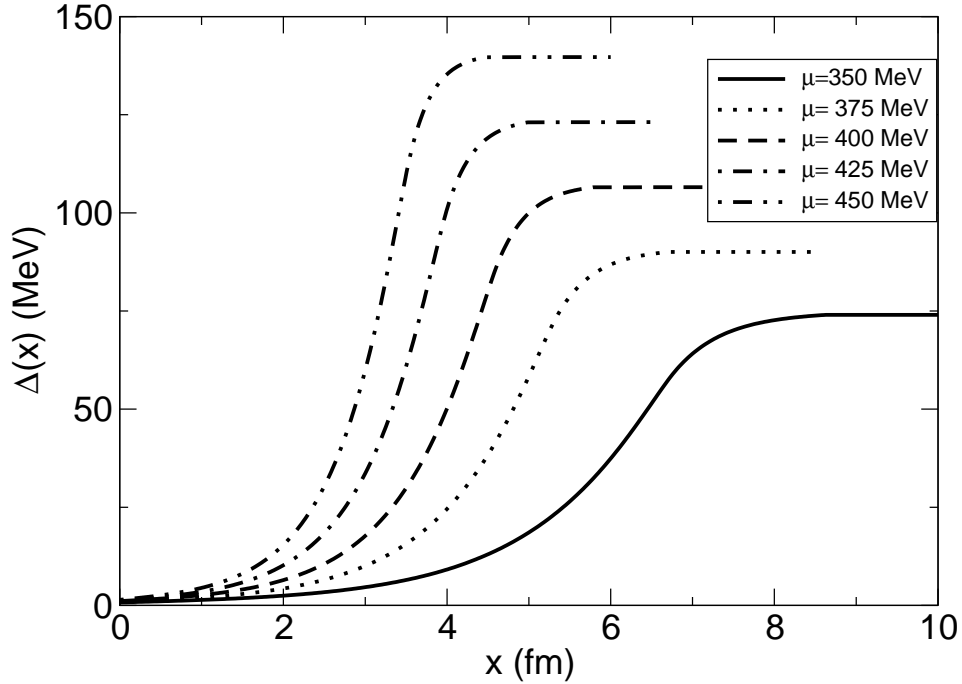


FIG. 2: The profile of  $\Delta(x)$  at the interface for various values of the baryon chemical potential.

We will now calculate the surface energy associated with the normal-superconductor interface. This will allow us to determine if the mixed phase is favored over the gapless state. To accomplish this we will need to allow for spatial variations of  $\Delta$  and calculate the gradient contribution to the free energy. We employ Landau-Ginsburg theory to do this. In their pioneering paper, Bailin and Love derive an expression for the gradient contribution to the free energy for a relativistic superconductor [2]. We will use this estimate, properly normalized for the 2SC case in what follows. The  $\Delta$  dependent contribution to the free energy of the 2SC phase, including the gradient terms, is given by

$$\mathcal{F}(\Delta)_{2SC} = \kappa_{2SC} |\nabla \Delta(x)|^2 + \Omega_{2SC}, \quad (18)$$

$$\text{where } \kappa_{2SC} = \frac{7\zeta(3)}{24\pi^4} \frac{\mu^2}{\alpha^2 \Delta_0^2}, \quad (19)$$

$\alpha \simeq 0.57 = k_B T_C / \Delta_0$ ,  $\zeta(3) \simeq 1.202$  and  $T_C$  is the BCS critical temperature. The contribution to the free energy which is independent of spatial derivatives is given by  $\Omega_{2SC}(\Delta)$  and was derived earlier in Eq. 8. In general, both the gradient term and  $\Omega_{2SC}$  are functions of all three chemical potentials, namely:  $\mu$ ,  $\mu_Q$  and  $\mu_8$ . While we retain this full dependence in  $\Omega_{2SC}$  as discussed earlier. We keep only the leading  $\mu$  dependence for the gradient term. We will later relax this assumption and study how these corrections will influence the surface tension. For now we shall proceed with the free energy given in Eq.19.

To construct the spatial profile of  $\Delta$  between the normal and superconducting phases we use the equation of motion. In one spatial dimension this is given by

$$\kappa_{2SC} \frac{d^2 \Delta(x)}{dx^2} = \frac{\partial \Omega_{2SC}}{\partial \Delta}. \quad (20)$$

We solve this ordinary differential equation subject to the boundary condition that  $\Delta(x=0) = 0$  and  $\Delta(x) = \Delta_0$  at large  $x$ . The results are shown in Fig. 20, where we calculate the interface for various values of the baryon chemical potential in the range  $\mu = 350 - 450$  MeV. The typical length scale for the variation of  $\Delta$  decreases with increasing  $\mu$  and  $\Delta$ . It ranges from about 3 fm at  $\mu = 350$  MeV to about 1 fm at  $\mu = 450$  MeV. Using these profiles, we have computed the surface tension by integrating the free energy function given in Eq. 19. The results are presented in the table below.

$\mu$ (MeV)	$\sigma$ (MeV/fm <sup>2</sup> )	$\mu$ (MeV)	$\sigma$ (MeV/fm <sup>2</sup> )	$\mu$ (MeV)	$\sigma$ (MeV/fm <sup>2</sup> )
350	1.6	375	3.8	400	6.8
425	10.9	450	16.6		

As mentioned earlier, the coefficient of the kinetic term, which we call  $\kappa_{2SC}$  ignores corrections due to  $\delta\mu$  and is based on the weak-coupling Landau-Ginsburg theory derived earlier [2]. We have examined how changes in  $\kappa_{2SC}$  would affect our calculation of the surface tension. We find that these changes are modest. The surface tension  $\sigma$  increased by 40% when  $\kappa_{2SC}$  was increased by a factor of two.

## V. PHASE DIAGRAM

Using the results of the previous sections, we can study the free energy competition between the gapless and mixed phases. The free energy of the mixed phase, including Coulomb and surface contributions is

$$\Omega_{\text{mixed}}(\mu) = \Omega_{2SC}(\mu, \bar{\mu}_Q) + E^S + E^C \quad (21)$$

where the surface and Coulomb contributions were defined in Eq. 17 and  $\bar{\mu}_Q$  is defined through Eq. 11. The left panel of the Fig. 3 shows the free energy difference  $\Delta\Omega = \Omega_{\text{gapless}} - \Omega_{\text{mixed}}$  for various values of the surface tension in the mixed phase. We have used this information in constructing the "phase diagram" as a function of  $\mu$  and  $\sigma$ , and is shown in the right panel of the figure. As expected, the gapless homogeneous phase is favored when  $\sigma$  is large and the mixed phase is favored for small  $\sigma$ . The surface tension computed in the previous section is also shown (filled circles). Their low values indicate that the mixed phase is favored.

We now examine if the assumptions made earlier in constructing the mixed phase are satisfied for the values of the surface tension calculated in Sec. IV. The Debye screening length in the normal and superconducting phases are easily computed by using the relation  $\lambda_D^{-2} = 4\pi \alpha_{\text{em}} \partial^2 \Omega_{2SC} / \partial \mu_Q^2$ . For the individual phases to have uniform charge distributions, their spatial extents in the mixed phase must be small compared to the Debye screening length. The table below provides a comparison between these length scales at various values of the baryon chemical potential. The results are shown for the mixed phase with  $d = 3$ , corresponding to a spherical geometry for the Wigner-Seitz. In the table,  $\Delta_{\text{BCS}}$ ,  $\chi$ ,  $R_D$  and  $R_{\text{ws}}$  correspond to the gap in the BCS phase, the volume fraction of the BCS phase, the droplet radius and the radius of the Wigner-Seitz cell respectively. Further, we have also implicitly assumed that the interface thickness is small compared to  $R_D$  and  $R_{\text{ws}}$ . The thickness parameter  $t$ , defined to be the distance over which the gap falls by a factor of  $e \simeq 2.718$ , is also given in the table.

$\mu$ (MeV)	$\Delta_{\text{BCS}}$ (MeV)	$\chi$	$R_D$ (fm)	$R_{\text{ws}}$ (fm)	$\lambda_D^{\text{sc}}$ (fm)	$\lambda_D^{\text{normal}}$ (fm)	$t$ (fm)
350	74	0.44	6.2	8.1	7.1	5.1	2.8
400	106	0.65	5.8	6.8	6.0	4.5	1.8
450	140	0.77	4.8	5.2	5.2	4.0	1.3

The length scales shown in the above table are fairly compatible with our earlier assumptions. However, since the Debye screening length and the spatial extents are of similar size, the charge distribution in the mixed phase could differ from the simple profiles considered here. We will not consider these screening corrections in this work, but this issue clearly warrants further study.

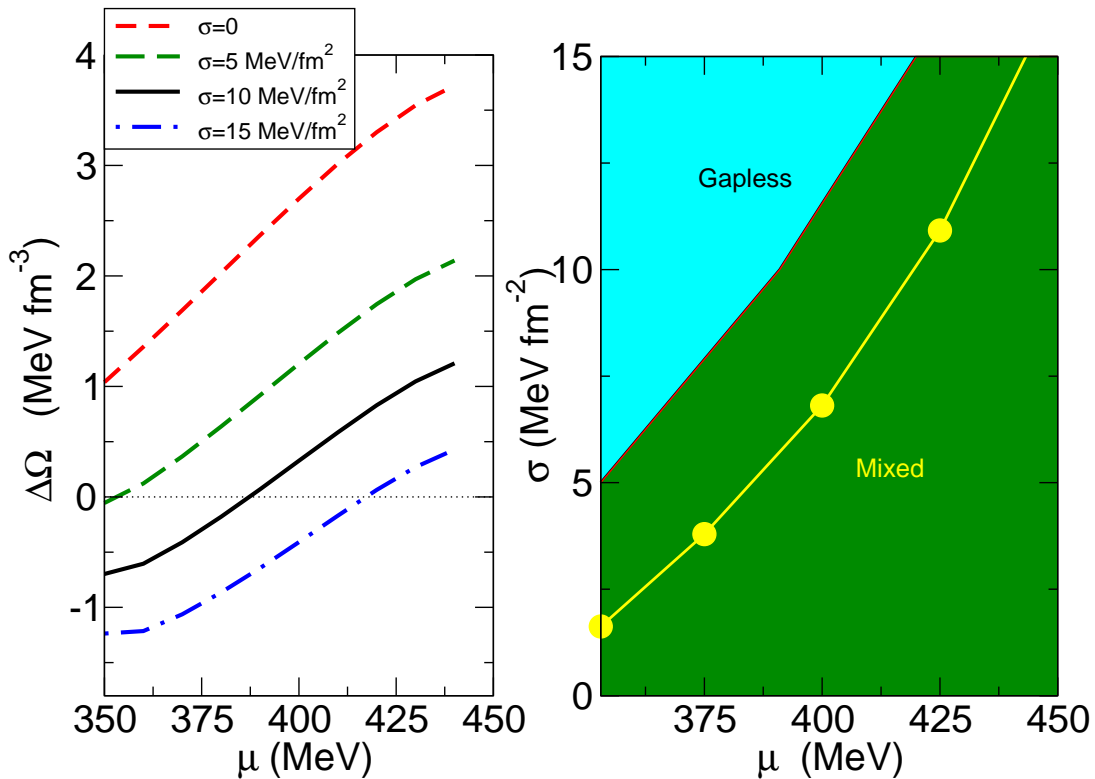


FIG. 3: Left panel: Influence of the surface energy on the total free energy difference between the gapless and mixed phases for various values of the surface tension. Right panel: The phase diagram showing the favored phase as a function of the surface tension and baryon chemical potential. The filled circles correspond to the results obtained from calculation of the surface tension outlined in Sec. IV.

## VI. DISCUSSION

Based on our calculation of the surface tension between normal and superconducting 2-flavor quark matter we have shown that a heterogeneous mixed phase is likely to be the ground state of quark matter at low density. The stress induced on the bulk system by the requirement of charge neutrality is resolved by phase separation. The other possibility, which is the homogeneous gapless phase exists as a local minima but is energetically disfavored. While we expect our qualitative results to be fairly robust, there are three important caveats to our finding that we shall now discuss. First of these caveats is related to the earlier observation that the surface thickness  $t \simeq 1 - 3 \text{ fm}$ , the typical physical sizes of the charged regions  $R_D \simeq 2 - 6 \text{ fm}$  and the Debye screening length  $\lambda_D \simeq 5 - 8 \text{ fm}$  are not well separated. This is likely to alter the simple structure of the mixed phase considered in this work. The charge, baryon density and the gap will vary smoothly over most of the Wigner-Seitz cell. These finite size corrections will need to be examined before one can draw firm conclusions regarding the phase competition (for a discussion of these effects in the context of a nuclear-kaon mixed phase see Ref. [17]). Second, we have assumed that the weak coupling BCS theory holds even when  $\Delta/\mu \simeq 1/3$ . In the BCS limit  $\Delta \ll \mu$ , neither the gapless nor the mixed phase could exist because for 2-flavor quark matter the electric charge chemical potential is proportional to the baryon chemical potential. In the strong coupling regime it is difficult to know a priori how other contributions to the free energy would alter this competition. Finally, we have used Landau-Ginsburg theory to calculate the coefficient of the gradient term in Eq. 19 to leading order. Strong coupling and the presence of electric charge chemical potential could modify this term and include higher order derivatives. However, as discussed earlier, even drastic changes to this coefficient (an increase by a factor of 2) resulted in a surface tension that continued to favor the mixed phase.

A heterogeneous quark matter ground state has important consequences for neutron star physics - were quark matter to exist inside their cores. The free energy difference between the gapless and mixed phase is small. Consequently, its effects on neutron star structure will be small. On the other hand, we can expect important changes to the transport properties induced by the heterogeneity of the mixed phase. In this phase, transport of the low energy neutrinos, photons, etc., will be dominated by coherent scattering induced by the presence of superconducting “bubbles” of quark matter with typical dimension of  $r_0 \simeq 5 \text{ fm}$  (for a discussion of how heterogeneity affects low energy neutrino transport see Ref. [18]). Further, the existence of regions with normal quark matter will affect the neutrino emissivities - since they are typically large in the normal phase. Finally, the

crystalline structure of the mixed phase could be relevant to the modeling of glitches observed in some pulsars.

We note that there are other mixed phases that could play a role in neutron stars. These include the mixed phase between quark matter and nuclear matter[14]; between color-flavor-locked matter and nuclear matter[19], or superconducting quark matter and normal quark matter[20]. All of these share several common features: the coexistence of positively and negatively charged phases separated by an interface; crystalline structure at low temperature; and coincidentally typical droplet sizes of the order 5 fm. However, in these forementioned examples it is still unclear if the mixed phase is favored when surface and Coulomb costs are included. This is because the surface tension is poorly known. Arguments based on naive dimensional analysis indicate that the surface energy cost may indeed be too large in these systems [19, 21].

Although quantitative aspects of the analysis presented in this work pertains to asymmetrical relativistic superconductors, our finding provide some qualitative insight into the behavior of non-relativistic superfluid that can be realized in ultra cold fermion-atom traps being developed in the laboratory. Although there is no Coulomb cost associated with the mixed state phase in these systems, a surface energy cost must be overcome when the surface to volume ratio is not negligible. The methods described in Sec. IV apply in general to asymmetrical fermion systems and its relevance to laboratory experiments is currently under investigation.

### Acknowledgments

We would like to thank Paulo Bedaque, Joe Carlson and Krishna Rajagopal for useful discussions. This research was supported by the Dept. of Energy under contract W-7405-ENG-36.

- 
- [1] B. C. Barrois, Nucl. Phys. **B129**, 390 (1977).
  - [2] D. Bailin and A. Love, Phys. Rept. **107**, 325 (1984).
  - [3] M. G. Alford, K. Rajagopal and F. Wilczek, Phys. Lett. **B422**, 247 (1998), [hep-ph/9711395].
  - [4] R. Rapp, T. Schafer, E. V. Shuryak and M. Velkovsky, Phys. Rev. Lett. **81**, 53 (1998), [hep-ph/9711396].
  - [5] M. G. Alford, K. Rajagopal and F. Wilczek, Nucl. Phys. **B537**, 443 (1999), [hep-ph/9804403].
  - [6] P. F. Bedaque and T. Schafer, Nucl. Phys. **A697**, 802 (2002), [hep-ph/0105150].
  - [7] D. B. Kaplan and S. Reddy, Phys. Rev. **D65**, 054042 (2002), [hep-ph/0107265].
  - [8] M. Alford, C. Kouvaris and K. Rajagopal, hep-ph/0311286.
  - [9] I. Shovkoy and M. Huang, Phys. Lett. **B564**, 205 (2003), [hep-ph/0302142].
  - [10] G. Sarma, Phys. Chem. Solid **24**, 1029 (1963).
  - [11] P. F. Bedaque, Nucl. Phys. **A697**, 569 (2002), [hep-ph/9910247].
  - [12] P. F. Bedaque, H. Caldas and G. Rupak, Phys. Rev. Lett. **91**, 247002 (2003), [cond-mat/0306694].
  - [13] M. G. Alford, J. A. Bowers and K. Rajagopal, Phys. Rev. **D63**, 074016 (2001), [hep-ph/0008208].
  - [14] N. K. Glendenning, Phys. Rev. **D46**, 1274 (1992).
  - [15] J. W. Negele and D. Vautherin, Nucl. Phys. **A207**, 298 (1973).
  - [16] D. G. Ravenhall, C. J. Pethick and J. R. Wilson, Phys. Rev. Lett. **50**, 2066 (1983).
  - [17] T. Norsen and S. Reddy, Phys. Rev. **C63**, 065804 (2001), [nucl-th/0010075].
  - [18] S. Reddy, G. Bertsch and M. Prakash, Phys. Lett. **B475**, 1 (2000), [nucl-th/9909040].
  - [19] M. G. Alford, K. Rajagopal, S. Reddy and F. Wilczek, Phys. Rev. **D64**, 074017 (2001), [hep-ph/0105009].
  - [20] F. Neumann, M. Buballa and M. Oertel, Nucl. Phys. **A714**, 481 (2003), [hep-ph/0210078].
  - [21] H. Heiselberg, C. J. Pethick and E. F. Staubo, Phys. Rev. Lett. **70**, 1355 (1993).